 doi:10.20944/preprints202009.0280.v1

Altered Spatial Composition of the Immune Cell Repertoire in the Bone Marrow Stem Cell Niche in Myelodysplastic Syndromes and Secondary Acute Myeloid Leukemia

Marcus Bauer[1#], Christoforos Vaxevanis[2#], Haifa Kathrin Al-Ali[3,4], Nadja Jaekel[3], Christin Le Hoa Naumann[3], Judith Schaffrath[3], Achim Rau [5], Barbara Seliger[2*], Claudia Wickenhauser[1*]

[1] Institute of Pathology, Martin Luther University Halle-Wittenberg, 06112 Halle, Germany

[2] Institute of Medical Immunology, Martin Luther University Halle-Wittenberg, 06112 Halle, Germany

[3] Department of Hematology/Oncology, University Hospital Halle, 06112 Halle (Saale), Germany

[4] Krukenberg Cancer Center, University Hospital Halle, 06112 Halle (Saale), Germany

[5] Institute of Pathology and Neuropathology, University of Tübingen, Tübingen, Germany

*shared senior authorship

shared first authorship

Corresponding author: Prof. Dr. Claudia Wickenhauser

Martin Luther University Halle-Wittenberg

Institute of Pathology

Magdeburger Str. 14

06112 Halle (Saale)

Germany

Telephone: (+49) (345) 557 - 1281

Fax: (+49) (345) 557 - 1295

E-mail: claudia.wickenhauser@uk-halle.de

 doi:10.20944/preprints202009.0280.v1

Additional information:

Running title: Multiplex immunohistochemistry of MDS and sAML bone marrow

Keywords: MDS, immune cell repertoire, prognosis, multiplex immunohistochemistry, stem cell niche

Financial support: The study was funded by Medicine Faculty of Martin Luther University Halle-Wittenberg as part of the Wilhelm-Roux-program (Project TIF 30/40).

Conflicts of interest: The authors declare no conflict of interest.

Acknowledgements: We would like to thank the Medicine Faculty of Martin Luther University Halle-Wittenberg for funding the study as part of the Wilhelm-Roux-program (Project TIF 30/40). We appreciate the support of Christiane Höfers for supporting the cytogenetic data. We would like to thank Sarah Vogtländer and Janin Siebert for excellent support in the laboratory, and Maria Heise and Vanessa Goldhorn for excellent secretarial help.

Word count: 5117

Total number of figures and tables: 2 tables, 5 figures

Preprints (www.preprints.org) | NOT PEER-REVIEWED | Posted: 13 September 2020 doi:10.20944/preprints202009.0280.v1

Translational relevance:

Despite a relationship between immune dysregulation and the course of MDS has been discussed, a detailed understanding of the role of immune cell subpopulations in this disease is still missing. Here, we present results of multiplex analyses of bone marrow samples from patients with myelodysplastic syndrome and secondary acute myeloid leukemia in order to determine the composition of immune cells and their localization in the bone marrow niche. Next to a high inter-tumoral heterogeneity of T and B cell populations and $CD34^+$ blasts in MDS and sAML, a distinct spatial distribution of B cells and an altered frequency of T cells were identified in the proximity to $CD34^+$ blasts in MDS and sAML independent of the clinical features and genetic alterations of the patients. Altogether, the correlative study suggests that MDS and sAML might have defective stem cell properties.

 doi:10.20944/preprints202009.0280.v1

Abbreviations

AML, acute myeloid leukemia; BM, bone marrow; BMB, bone marrow biopsy; CCSS, Comprehensive Cytogenetic Scoring System; CTL, cytotoxic T lymphocyte; dcc, direct cellular contact; EB, excess of blasts; FFPE, formalin fixed and paraffin embedded; HC, healthy control; HMA, hypomethylating agents; HSC, hematopoietic stem cell; HSPC, hematopoietic stem and progenitor cell; IGH, immunoglobulin heavy chain; IHC, immunohistochemistry; IPSS-R, Revised International Prognostic Scoring System; mAb, monoclonal antibody; MDS, myelodysplastic syndrome; MSC, mesenchymal stem cell; MSI, multispectral imaging; NGS, next generation sequencing; sAML, secondary acute myeloid leukemia; TLR, toll-like receptor; TME, tumor microenvironment; Treg, regulatory T cell; TSA, Tyramide signal amplification; WHO, World Health Organization

Preprints (www.preprints.org) | NOT PEER-REVIEWED | Posted: 13 September 2020 doi:10.20944/preprints202009.0280.v1

Abstract

Purpose: Myelodysplastic syndromes (MDS) are caused by a stem cell failure, but the relationship between immune dysregulation and the course of disease has not yet been analyzed in detail.

Experimental design: To get insights into the pathophysiologic and clinical relevance of the histotopography of immune cell subpopulations in this process, the immune cell infiltrate with focus on its spatial distribution was determined by multispectral imaging (MSI) in 147 bone marrow biopsies from MDS or secondary acute myeloid leukemia (sAML) patients and healthy controls (HC). In addition, the data were correlated to genetic alterations and clinical features of these patients including therapy response.

Results: A high inter-tumoral heterogeneity in the frequency and spatial distribution of $CD3^+CD8^+$, $CD3^+CD8^-$, $CD3^+FOXP3^+$ T cell subsets, $MUM1p^+CD3^-$ post-germinal B/plasma cells and $CD34^+$ blasts was found in MDS and sAML samples. In HC only few B cells/plasma cells, but no T cell subpopulations were detected in the proximity to $CD34^+$ blasts. In contrast, the frequency of these lymphocytes was increased in proximity to $CD34^+$ blasts in both MDS and sAML independent of the karyotype, genetic alterations frequently detected in MDS, clinical risk stratification systems or treatment response to hypomethylating agents. Furthermore, an increased frequency of $CD3^+CD8^+$ T cells and $MUM1p^+$ $CD3^-$ B cells was found in responders to epigenetic drugs.

Conclusions: Thus, we conclude that (i) T cell subsets do not belong to the normal stem cell niche, (ii) the presence of T and B cell subpopulations not directly affect the course of MDS, (iii) lymphocytes in the proximity to $CD34^+$ blasts might indicate defective stem cell properties and (iv) the number of lymphocytes is a predictor of therapy response to hypomethylating agents.

Preprints (www.preprints.org) | NOT PEER-REVIEWED | Posted: 13 September 2020 doi:10.20944/preprints202009.0280.v1

Introduction

Myelodysplastic syndromes (MDS) are heterogeneous clonal hematologic diseases characterized by an ineffective hematopoiesis, one or more lineage dysplasia and peripheral cytopenia (1–3). Multifactorial pathogenic features with diverse cytogenetic, molecular and epigenetic alterations are associated with a variable clinical presentation (4,5). Chronic inflammatory diseases associated with activated immune signaling pathways often precede the clinical manifestation of MDS suggesting an aetiopathogenetic link between chronic immune signaling, impaired stem cell quality and alteration of the stem cell microenvironment (6). There is growing evidence of immune dysregulation during the course of this disease (7,8), such as overexpression of immune-related genes in hematopoietic stem and progenitor cells (HSPC) (9,10). However, the interrelationship between chronic immunologic stimulation and initiation as well as progression of MDS to secondary acute myeloid leukemia (sAML) remains largely unknown. Thus, a connection between immune dysregulation (11–13) and established prognostic parameters, such as bone marrow (BM) blast count, cytogenetic alterations and the degree of peripheral cytopenia, which are all integrated in the Revised International Prognostic Score System (IPSS-R) (5,14), might contribute to a better understanding of pathogenesis and the consequence of altered immunologic features in this disease.

Low risk MDS are related to higher levels of $CD8^+$ cytotoxic T lymphocytes (CTL) and lower levels of $FoxP3^+$ regulatory T cells (Treg), while the frequency of both CTL and Treg is inversely correlated in high risk MDS (15–19). In addition, deregulated innate immune responses have an important impact on the pathogenesis of MDS (20–22) with a significantly higher somatic hypermutation rate of immunoglobulin heavy chain (IGH) clones in BM cells from del(5q) MDS patients indicating an extended number of antigen experienced B cells (23).

To get in depth insights into the risk dependent deregulation of the immune cell subpopulations in MDS and sAML, a six-color multispectral imaging (MSI) panel was established and the frequency of immune cell subpopulations, their spatial distribution and the probability of the cellular interaction was analyzed in 147 bone marrow biopsies (BMB) from MDS and sAML patients as well as healthy controls (HC) correlated to characteristics.

Preprints (www.preprints.org) | NOT PEER-REVIEWED | Posted: 13 September 2020 doi:10.20944/preprints202009.0280.v1

Materials and methods

Patient characteristics

Bone marrow biopsies (BMB) collected between 2014 and 2019 at the Medical Faculty of the Martin-Luther University Halle-Wittenberg, Germany, were part of the routine diagnostic approach based on screening and/or treating patients within clinical trials. The cohort comprised BMB of 102 patients divided in 69 MDS patients with different blast counts (without and with excess of blasts (EB-1-2)) and 33 BMB of sAML patients. All BMB were evaluated regarding their clinico-pathological characteristics as summarized in Table 1. Further, 45 BMB from age-matched patients with normal blood cell count and without evidence of myeloid or lymphoid neoplasia served as HC.

Clinical, laboratory, molecular and cytogenetic data including the CCSS, risk group according the IPSS-R and treatment data were collected from the medical records. MDS patients were stratified into the following disease groups: MDS without EB (<5% blasts), MDS with EB-1 (MDS-EB-1, 5-9.9% blasts), MDS with EB-2 (MDS-EB-2, 10-19.9% blasts) and sAML (≥20% blasts) based on the cytological blast count. sAML patients were further divided in two groups characterized by BM blast counts of 20-29.9% and higher than 30%.

Study approval

Informed consent was obtained from all patients and HC for the use of their diagnostic material for scientific research, which was approved by the Ethical Committee of the Medical Faculty of the Martin Luther University Halle-Wittenberg, Halle, Germany (2017-81). In addition, the same Ethical Committee approved the scientific use of formalin fixed and paraffin embedded (FFPE) samples.

Standard morphological evaluation of the bone marrow

Diagnosis of MDS and sAML with myelodysplasia related changes was performed according to the diagnostic criteria of the WHO classification of Tumors of Hematopoietic and Lymphoid tissues, 4th edition 2017 (24).

Preprints (www.preprints.org) | NOT PEER-REVIEWED | Posted: 13 September 2020 doi:10.20944/preprints202009.0280.v1

To confirm the diagnosis of MDS and sAML, conventional histological and cytological examination as well as immunohistochemistry (IHC) was performed. Monoclonal antibodies (mAb) directed against CD34 (clone QBend/10, Labvision, Germany), CD117 (clone CD117, c-kit A4502, Dako, USA), MPO (clone myeloperoxidase A0398, Dako, USA), lysozyme (EP134, Epitomics, USA), and CD71 (MRQ-48, Cell Marque, USA) were used according to the supplier's instructions.

Multispectral Imaging (MSI)

The frequency, localization and spatial proximity of immune cell subpopulations and $CD34^+$ blasts were analyzed by multispectral imaging (MSI). The staining procedure was performed as recently described (25,26) using mAb directed against CD34 (QBend, Labvision, Germany, 1:500, pH6), CD3 (Labvision, Germany, clone SP7), CD8 (Abcam, UK, clone SP16), FOXP3 (Abcam, UK, clone 236A/E7), and MUM1p (Dako, USA, cloneMUM1p). Briefly, all primary mAb were incubated for 30 minutes. Tyramide signal amplification (TSA) visualization was performed using the Opal seven-color IHC Kit containing fluorophores DAPI, Opal 540, Opal 570, Opal 620, Opal 650, Opal 690 (PerkinElmer Inc., USA). Stained slides were imaged employing the PerkinElmer Vectra Polaris platform. To unify the spatial distribution analysis three ×20 MSI fields (1872 x 1404 pixel, 0.5 µm/pixel) were manually selected on each slide based on representativeness and tissue size. Since the BMBs showed a high range in quality and size, areas with preserved architecture were chosen, while hemorrhagic areas and areas with artificial lacks were excluded. Cell segmentation and phenotyping were performed using the inForm software (PerkinElmer Inc., USA). The frequency of all immune cell populations analyzed and the cartographic coordinates of each stained cell type were obtained. The spatial distribution was analyzed using PerkinElmer inform and R script for immune cell enumeration and relationship analysis. The performed multiplex staining panel allowed to differentiate the distinct T cell subpopulations $CD3^+CD8^+$ T cells, $CD3^+CD8^-$ T cells and $CD3^+FOXP3^+$ T cells, respectively. Due to the limited number of T cell markers only broad T cell subsets were distinguished: $CD3^+CD8^+$ T cells were classified as CTL and $CD3^+FOXP3^+$ T cells as Treg. All

Preprints (www.preprints.org) | NOT PEER-REVIEWED | Posted: 13 September 2020 doi:10.20944/preprints202009.0280.v1

MUM1p$^+$ B cells/plasma cells lack CD3 expression. CD34$^+$ blast cells were separated from CD34$^+$ endothelial cells by histomorphology based on their localization and cytological appearance.

Mutational analysis - targeted Next Generation Sequencing

Targeted mutation analyses were performed by Next Generation Sequencing (NGS; Ion GeneStudio S5 prime, Thermo Fisher Scientific, Waltham, MA, USA) using an AmpliSeq Custom Panel designed for myeloid disorders comprising hotspot regions in 21 genes (JAK2, FLT3, STAT3, ASXL1, IDH1, IDH2, SRSF2, SF3B1, U2AF1, SETBP1, MPL, KIT, CBL, CSF3R, CALR, ETNK1, KRAS, NRAS, HRAS, BRAF, GNAS) and the 10 genes (CEBPA, RUNX1, IKZF1, DNMT3A, EZH2, ZRSR2, TP53, TET2, NPM1, STAG2). Amplicon library preparation and semiconductor sequencing was done according to the manufacturers' manuals using the Ion AmpliSeq Library Kit v2.0, the Ion Library TaqMan Quantitation Kit, the Ion 510 & Ion 520 & Ion 530 Kit – Chef and the Ion 520 Chip Kit (Thermo Fisher Scientific).

Variant calling of non-synonymous somatic variants compared to the human reference sequence was performed using Ion Reporter Software (Thermo Fisher Scientific, Version 5.12.3.0). Variants were filtered with a threshold allele frequency of 5%.

Variants called by the Ion Reporter Software were visualized using the Integrative Genomics Viewer (IGV; Broad Institute, Cambridge, MA; Version 2.5.2) to exclude panel-specific artefacts.

Statistics and software

Statistical analyses were performed employing IBM SPSS Statistics. Kolmogorov-Smirnov test revealed non-parametric data ($p<0.05$). The Mann-Whitney U test was employed to compare clinical data, frequencies of immune cell subpopulations and their spatial distribution. P values <0.05 were considered statistically significant.

The figures were generated using the graphpad Prismen 7.0 software.

Preprints (www.preprints.org) | NOT PEER-REVIEWED | Posted: 13 September 2020 doi:10.20944/preprints202009.0280.v1

Results

Establishment of the MSI technology on decalcified BMB

In order to determine the composition and spatial distribution of immune cell subpopulations in BMB, the MSI technology was first adapted to decalcified FFPE tissue samples. BMB from 45 HC as well as 69 MDS and 33 sAML patients were analyzed by simultaneous staining for the markers CD3, CD8, FOXP3, MUM1p and CD34, combined with nuclear staining using DAPI as representatively shown in Figure 1 a-d. One analyzed MSI field (1872 x 1404 pixel, 0.5 µm/pixel) contained a mean of 3495 cells in BMB of HC, 3694 cells in BMB of MDS unseparated for blast count (average 3393 cells in MDS without EB, average 3836 cells in MDS-EB-1, and average 4067 cells in MDS-EB-2) and of 5429 cells in BMB of sAML with a maximum of 9297 cells/MSI field. Within the BMB of HC, the blast counts varied between 0.7-1.8%. Four distinct immune cell subpopulations could be separated: $CD3^+CD8^+$ T cells, $CD3^+CD8^-FOXP3^-$ T cells (T helper cells, and/or NKT cells), $CD3^+FOXP3^+$ T cells and $MUM1p^+CD3^-$ post-germinal center B/plasma cells. The frequency of the different immune cell subsets in HC, MDS without EB, EB 1-2 and sAML samples unselected for cytogenetic aberrations or treatment was comparable between the three categories (Figure 3).

Differences in the frequency and histotopography of immune cell subsets in spatial relationship with $CD34^+$ blasts in MDS, sAML and HC

Since the MSI technology allows the determination of the spatial distribution between cell populations, the distances between different immune cell subsets and $CD34^+$ blasts were analyzed and categorized as (I) direct cellular contact (dcc), (II) cells within a radius of 10 µm, (III) cells within a radius of 25 µm and (IV) cells within a radius of 50 µm (Figure 1e-f).

The histotopography of the immune cell subsets demonstrated a complete absence of $CD3^+FOXP3^+$ T cells within a distance of <25 µm (p=0.000) and only very few $CD3^+CD8^+$ T cells within a 25 µm radius (p=0.000) and from $CD34^+$ blasts, but not in dcc or the 10 µm radius were found in all HC (Figure 2 and 3). In addition, the frequency of $MUM1p^+CD3^-$ B cells in the

Preprints (www.preprints.org) | NOT PEER-REVIEWED | Posted: 13 September 2020 doi:10.20944/preprints202009.0280.v1

proximity of $CD34^+$ blasts was significantly lower (p=0.000) for all categories [I-IV] in HC (Figure 3).

By grouping untreated MDS and sAML patients, a higher frequency of different immune cell subpopulations in proximity to $CD34^+$ blasts was detected in the sAML patients. This effect was most pronounced for $CD3^+CD8^+$ T cells with an average of 0.33 $CD3^+CD8^+$ T cells within a 10 µm radius around $CD34^+$ blasts in sAML and an average of 0.08 $CD3^+CD8^+$ T cells in MDS samples (p=0.007). Furthermore, an average of 0,25 $CD3^+FOXP3^+$ T cells was detected within a 10 µm radius around $CD34^+$ blasts in sAML samples when compared to an average of 0.12 $CD3^+FOXP3^+$ T cells in MDS (p=0.07) (Figure 3).

Correlation of the frequency and histotopography of immune cell subsets with blast cell count in MDS and sAML

To exclude that differences in the inflammatory cell distribution were an effect of BM cellularity, BMB of HC and MDS patients without EB were compared. MDS samples without EB (average 3694 cells) presented a comparable BM cellularity to HC (average 3495 cells), but had significantly higher T cell counts in proximity to $CD34^+$ cells with 2 $CD3^+CD8^+$ T cells and 1.5 $CD3^+FOXP3^+$ T cells next to $CD34^+$ blasts within the 10 µm radius. In contrast, a complete absence of $CD3^+FOXP3^+$ T cells and only a few $CD3^+CD8^+$ T cells within a distance of < 25 µm to $CD34^+$ blasts were found in HC (Figure 2 and 3).

Comparing BMB of HC and MDS / sAML patients, only minor differences in the frequencies of respective immune cell subsets were found (Figure 3a), while in contrast to HC the analyses of the spatial distribution of BMB demonstrated immune cell subpopulations in close proximity to $CD34^+$ blasts. MDS patients and patients with sAML < 30% blasts had a comparable frequency of $CD3^+FOXP3^+$ T cells, $CD3^+CD8^+$ T cells and $MUM1p^+CD3^-$ B/plasma cells, but the number of $CD3^+CD8^+$ T cells next to $CD34^+$ blasts was slightly increased in sAML < 30% blasts. A significant increase (p=0.022) in $CD3^+CD8^+$ T cells was found in sAML samples with $CD34^+$ blast counts >30% when compared to other disease groups and to HC (Figure 3b-c).

Preprints (www.preprints.org) | NOT PEER-REVIEWED | Posted: 13 September 2020 doi:10.20944/preprints202009.0280.v1

Influence of the frequency and histotopography of the immune cell subsets by the cytogenetic score in MDS

Based on the cytogenetic aberrations in MDS without EB and EB 1-2, patients were classified according to the CCSS (14) and the respective subgroups were compared (Table 1). The lower risk subgroup comprised samples with very low and low risk cytogenetic aberrations (CCSS 1-2), while diseases with intermediate, high, and very high cytogenetic scores were defined as higher risk subgroup (CCSS 3-5). The frequency of $CD3^+FOXP3^+$ T cells and $MUM1p^+CD3^-$ B/plasma cells was significantly higher in CCSS high risk cases compared to CCSS low risk cases (p=0.042; p=0.004; Figure 4a). No significant differences in the frequency of $CD3^+CD8^+$ and $CD3^+CD8^-$ T cells were detected between CCSS low risk, CCSS high risk and HC cases (Figure 4a). Furthermore, no significant differences in the frequency of T cell and $MUM1p^+CD3^-$ B/plasma cell subpopulations were detected in patients with normal or abnormal karyotypes.

To determine the impact of the CCSS on the composition and the histotopography of the immune cell repertoire, the spatial proximity of respective phenotypes was calculated for all four proximity categories demonstrating no significant differences regarding the direct and close contact of immune cell subsets and $CD34^+$ blasts (Figure 4b). However, significant more $MUM1p^+CD3^-$ B/plasma cells were detected within a 25 µm radius (p=0.0012) and increased numbers of $CD3^+CD8^+$ T cells within the 25 µm radius of the $CD34^+$ blasts in the higher risk subgroup (p=0.099).

Effect of the mutational status in MDS on the frequency and histotopography of the immune cell subsets

In order to investigate whether structural alterations in MDS samples have an effect on the immune cell composition of the BM, targeted NGS was carried out on the samples of MDS (n=28) and sAML (n=10) patients. As shown in Table 2, mutations in the samples were detected in 10/22 genes analysed in particular in genes involved in the epigenetic regulation, signal transduction, transcription and DNA repair with the highest frequency of mutations in TP53 (10/28). The frequency of mutations detected in the MDS patients was heterogeneous

Preprints (www.preprints.org) | NOT PEER-REVIEWED | Posted: 13 September 2020 doi:10.20944/preprints202009.0280.v1

varying from five mutations in one to no mutation in three out of 28 patients, while in 50% of MDS patients one mutation was (Table 2).

Apart from patients with mutations in genes coding for proteins involved in the signal transduction, that showed increased frequencies of $CD3^+CD8^+$ T cells (p=0.058) and $CD3^+FOXP3^+$ T cells (p=0.021) and a slight, but not significantly increased proportion of $CD3^+CD8^-$ T cells in patients with mutations in splicing factors (p=0.053), neither significant differences in the frequency nor in the spatial distribution of the immune cell subpopulations in relation to $CD34^+$ blasts were detected. In contrast, in patients harboring one or more mutations in splicing factors, chromatin modification, and DNA methylation, $CD3^+CD8^-$ T cells and $CD3^+FOXP3^+$ T cells are more often in close proximity in all distance categories (p=0.017). No significant association of the mutational status and the progression to sAML was detected. However, patients that responded to treatment with hypomethylating agents showed mutations exclusively in IDH1, IDH2, TET2, ASXL1, and SRSF2 and had a lower frequency of TP53 mutations (55.0% vs. 80.0%).

Spatial distribution of immune cell subsets and $CD34^+$ blasts in relation to MDS progression to sAML

A possible prognostic value of the immune cell landscape in association with $CD34^+$ cells was postulated. Indeed, patients with a higher IPSS-R (intermediate, high and very high risk) showed increased frequencies of $CD3^+FOXP3^+$ T cells (p=0.004) and $MUM1p^+CD3^-$ B/plasma cells (p=0.062) in the BM (Figure 4c). Concerning the spatial distribution increased numbers of $CD3^+FOXP3^+$ T cells within a 10 µm radius of $CD34^+$ blasts (p=0.05) and $CD3^+CD8^+$ T cells (p=0.09) were found (Figure 4d). To exclude therapy effects, patients with comparable clinic-pathologic characteristics and neither treatment with HMA nor allogeneic stem cell transplantation were separated into those patients with (n=6) and without (n=29) progress to sAML in the course of MDS (Table 1). While the mean frequency of T cell subsets was comparable in the two subgroups (Figure 5a), the frequency of $MUM1p^+CD3^-$ B/plasma cells was significantly higher in patients with disease progression (p=0.033). However, no significant

Preprints (www.preprints.org) | NOT PEER-REVIEWED | Posted: 13 September 2020 doi:10.20944/preprints202009.0280.v1

differences in the spatial distribution of the immune cells in relation to the $CD34^+$ blasts as well as to the respective immune cell subsets were found (Figure 5b).

Prediction of treatment response to hypomethylating agents by the frequency of immune cell subsets and immune cell subpopulations proximity

To predict therapy response to hypomethylating agents, patients were divided into responders (n=12) and non-responders (n=5) depending on the blast count in the course of the disease. While the frequency of $CD3^+$ T cells (7.7% versus 6.4%) mainly consisting of $CD3^+CD8^-$ T cells (4,2% versus 2,0%) was higher in patients responding to hypomethylating agents, the number of $CD3^+CD8^+$ T cells was slightly, but not significantly higher in the group of non-responders (Figure 5c).

Responders to hypomethylating therapy exhibited a significant higher frequency of $CD3^+$ $CD8^-$ T cells in the neighborhood of $CD3^+CD8^+$ T cells (p=0.011) (Figure 5d), which was comparable to that of HC. Furthermore, significant more $MUM1p^+CD3^-$ B/plasma cells were found within a 25 µm radius of $CD3^+$ T cells (p=0.025). No significant differences of the immune cell infiltrates in the proximity of $CD34^+$ blasts were found.

Preprints (www.preprints.org) | NOT PEER-REVIEWED | Posted: 13 September 2020 doi:10.20944/preprints202009.0280.v1

Discussion

Immune dysregulation plays a key role in MDS and is linked to the disease initiation and progression to sAML (27,28). So far, most studies analyzed the influence of the innate immune response in MDS and sAML (15), in particular impaired Toll-like receptor (TLR) signaling pathways due to overexpression and/or mutations in related genes and microRNAs (28). Furthermore, a high frequency of mutations in DNMT3A, TET2, and ASXL1 has been identified in MDS and sAML, which influence the innate immune signaling through various mechanisms (29). In contrast, only limited information concerning the adaptive immune system exists, despite its reported activation in the neoplastic stem cell niche of MDS (15). Flow cytometric analyses demonstrated a dynamic immune cell repertoire with a higher frequency of NK cells and CTL in lower risk MDS patients when compared to controls, while an increased Treg frequency was found in high-risk MDS patients (17,19). Since interactions of adaptive immune cells might affect the initiation, progression and therapy response in MDS, in depth analyses of the immune cell subpopulations and their interactions with hematopoietic cells were performed in this study.

For characterization of the immune cell composition and the spatial distribution, the MSI technology was modified for the use on decalcified FFPE BMB samples. However, so far there exists no general information, about which spatial distances between immune cell subsets and in relation to tumor cells are of biologically relevance in hematologic malignancies. In solid tumors, a prognostic impact of tumor and immune cell proximity was shown within an intercellular distance of 20 – 30 µm (30,31), In this study, most significant differences in the samples analyzed regarding immune cell subsets and blasts were found within a distance of <10 µm suggesting a biological relevance.

The number of different immune cell subpopulations in relation to the entire BM cells varied in BMB of HC and diseased patients from MDS / sAML. The complete absence of the T cell subsets analysed and a highly significant lower frequency of MUM1p^{+}CD3^{-} B/plasma cells within a radius of <50 µm in samples from HC compared to diseased BMB, could not be explained by a lower BM cellularity in HC underlining the methodological strength and

advantage of the MSI approach in comparison to cytomorphological and/or immunological analysis of fluid BM cells.

The complete absence of any T cell subsets in the neighborhood of $CD34^+$ cells postulated that these immune cell subpopulations are not common components of the normal HSC niche mainly consisting of mesenchymal cells (32–38). Vice versa, the presence of these immune cell subsets within the $CD34^+$ stem cell niche in the BM of MDS and sAML patients indicates a role of these cells in the pathogenesis of these diseases and are in accordance with accumulating evidence identifying the BM microenvironment as a regulator of the neoplastic stem cell pool and key mediator of MDS pathophysiology (33,35,36,38). Based on xenograft models, MDS cells require support from microenvironmental components to propagate disease. Furthermore, MDS-derived mesenchymal stem cells are molecularly distinct from their healthy counterparts in terms of their gene expression profiles (37), in particular of inflammation-associated genes implicated in inhibition of hematopoiesis (39). In addition, MDS initiation is influenced by extrinsic defects of osteoprogenitors with an altered ribosome biogenesis and ribsomopathy including excess of ribosomal-free ribosomal proteins (40). The latter can participate in innate as well as interferon-γ (IFN-γ)-mediated inflammatory responses by selectively modulating e.g. the NF-κB target gene expression. Together, these observations postulated an ineffective hematopoiesis and leukemic progression of human MDS exclusively driven by hematopoietic cell autonomous events. However, our study demonstrates alterations in the cellular repertoire of the microenvironment beyond MSC and an interaction of different immune cell subpopulations as important players in the disease process. This is further substantiated by the fact that MDS frequently coexists with inflammatory disorders as rheumatoid arthritis frequently precedes MDS (41,42) and patients with autoimmune disorders or with chronic infections have an increased risk to develop MDS (11–13).

So far, the association between MDS and common genetic predispositions or pharmacological treatment is controversially discussed. Our study suggests that a local accumulation of inflammatory cells next to $CD34^+$ stem cells/progenitors may directly damage BM precursors, and drive malignant transformation. To further determine whether the local accumulation of T

cell subpopulations and MUM1p$^+$CD3$^-$ B cells/plasma cells might not only be associated with disease initiation, but also with disease progression, the density of the immune cell subsets from BMB of MDS and sAML patients was correlated to the CD34$^+$ blast cell content. Despite a comparable immune cell frequency next to CD34$^+$ cells in BMB of patients with MDS EB-0-2 and sAML <30% blast cell count, sAML patients with >30% blast content had significant elevated numbers of CD3$^+$CD8$^-$ T cells, CD3$^+$FOXP3$^+$ T cells and MUM1p$^+$CD3$^-$ B cells next to CD34$^+$ blasts, independent of an increased frequency of CD3$^+$FOXP3$^+$ T cells in the neighborhood of CD3$^+$CD8$^-$ T cells. Although the impact of this specific local immunological landscape remains unclear, sAML with a blast cell count of >20% and <30%, formerly also designated as RAEB-T, display a unique biologic entity with clinical features rather consistent with MDS than with AML (43).

Cytogenetic aberrations and frequently occurring mutations with known prognostic value in MDS might lead to the generation of neoantigens with the consecutive generation of antigen-specific immune responses in MDS and sAML. Significant higher levels of CD3$^+$FOXP3$^+$ T cells in patients with higher risk cytogenetic aberrations (CCSS score 3-5) were detected, which are associated with the presence of myeloid derived suppressor cells also known to contribute significantly to the dysregulation of immune surveillance in MDS (44). Despite a closer proximity of CD3$^+$CD8$^-$ T cells and CD3$^+$FOXP3$^+$ T cells in patients with mutations in epigenetic regulators, no significant differences in the spatial distribution of immune cell subpopulations were detectable. Since most of the mutations identified alter the adaptive rather than the innate immune signaling, we conclude that the presence of T and B subsets in close proximity to CD34$^+$ blasts in MDS and sAML is independent of karyotypic and mutational induced neoantigens associated with immune modulatory mechanisms (34,45).

Since the frequency of immune cell subsets and their topography within the BM cells might predict the response rate to HMA therapy currently used for the treatment of high-risk MDS or AML patients, the immune cell repertoire was associated with therapy response (46). Immune-mediated anti-tumoral effects of these drugs were described, such as an upregulation of tumor-associated antigens and HLA class I molecules, which is accompanied by an altered T and/or

Preprints (www.preprints.org) | NOT PEER-REVIEWED | Posted: 13 September 2020 doi:10.20944/preprints202009.0280.v1

NK cell functionality *in vitro* and *ex vivo (47)*. Furthermore, patients with an intermediate-2 or high-risk MDS responding to the hypomethylating treatment exhibit fewer Treg upon long-term follow-up compared to Treg frequencies of healthy donors (48). In our study, a higher proportion of $CD3^+$ T cells mainly consisting of $CD3^+CD8^-$ T cells was detected in responders to hypomethylating agents, while the number of $CD3^+CD8^+$ T cells was slightly, but not significantly higher in the group of non-responders. Patients responding to the hypomethylating therapy exhibited a lower number of $CD3^+FOXP3^+$ T cells neighboring $CD3^+$ T cells or $MUM1p^+CD3^-$ B/plasma cells and a higher number of $CD3^+CD8^-$ T cells in the neighborhood of $CD3^+CD8^+$ T cells. No significant differences of the immune cell infiltrate in the proximity of $CD34^+$ blasts were found. Thus, hypomethylating therapy caused changes within the local BM micromilieu of MDS / sAML patients with T cell interactions in the BMB of therapy responders resembling those of HC. Therefore, hypomethylating agents may act by modifying components of the adaptive immune system regarding the frequency and distribution of immune cells comparable to that in HC. This normalization does not include the stem cell niche, as hypomethylation therapy did not lead to the disappearance of the immune cell subsets in the neighborhood to $CD34^+$ stem cells, which is in line with the lack of elimination of the neoplastic clone in MDS and sAML by hypomethylating agents.

In conclusion, immune profiling of HSC niches and spatial immune cell interactions by MSI represents a powerful tool for investigating the clinical relevance of the frequency and the spatial distribution of immune cell subsets in healthy BMB, MDS, and sAML. However, further investigations to identify the underlying immune regulatory mechanisms and their importance for the design of potent immunotherapies in MDS and sAML are urgently needed.

Preprints (www.preprints.org) | NOT PEER-REVIEWED | Posted: 13 September 2020 doi:10.20944/preprints202009.0280.v1

Declarations

Ethics approval

Informed consent was obtained from all patients and HC for the use of their diagnostic material for scientific research, which was approved by the Ethical Committee of the Medical Faculty of the Martin Luther University Halle-Wittenberg, Halle, Germany (2017-81). In addition, the same Ethical Committee approved the scientific use of FFPE samples.

Consent for publication

All authors read the final version of the manuscript and gave their consent for publication.

Availability of data and material

For original data, please contact marcus.bauer@uk-halle.de.

Authors' contributions

All authors contributed to the contents and revised the article. M. B., C. V., N. J. and A. R. were responsible for the provision of data. C. W. and B. S. designed the study. M. B. and C. V. did the data analysis, interpreted the data, while M.B., C.V., C.W. and BS wrote the article.

Preprints (www.preprints.org) | NOT PEER-REVIEWED | Posted: 13 September 2020 doi:10.20944/preprints202009.0280.v1

Tables and figure legends

Table 1: **Clinico-pathological characteristics and sample specifications in terms of risk factors, treatment, and prognosis**

		MDS	sAML	HC
number of samples		69	33	45
age		68,2 (42-86)	68,9 (47-82)	59,6 (39-84)
sex	male	39	18	24
	female	30	15	21
MDS	without excess of blasts	22	-	-
	with excess of blasts 1 (EB-1)	26	-	-
	with excess of blasts 2 (EB-2)	21	-	-
CCSS	**1 -** loss of Y chromosome, del(11q)	7	2	-
	2 - normal karyotype, del(5q), del(12p), del(20q)	27	5	-
	3 - del(7q), gain of chromosome 8 and 19, isochromosome 17q	17	3	-
	4 - gain of chromosome 3 and 7, complex (>2)	1	2	-
	5 - complex (>3)	17	9	-
IPSS-R	**1** - very low risk	2	-	-
	2 - low risk	6	-	-
	3 - intermediate risk	20	-	-
	4 - high risk	26	-	-
	5 - very high risk	15	-	-
patients without therapy (neither allogeneic stemm cell transplantation nor HMA treatment)		35		
patients with prior treatment with HMA		17	6	-
patients with MDS with treatment response to HMA		12	-	-
patients that received allogeneic stem cell transplantation		23	9	-
MDS with further progress to sAML		18	-	-

Preprints (www.preprints.org) | NOT PEER-REVIEWED | Posted: 13 September 2020 doi:10.20944/preprints202009.0280.v1

Table 1: Landscape of mutations frequently detected and prognostic relevant in MDS and correlated to progress to sAML

Detected mutations are marked with asterisks (*). Twenty eight samples of patients with MDS were analyzed by targeted NGS as described in materials and methods. The frequency of mutations is shown as numbers and percentage. The mutations are shown in correlation to the cytogenetic aberrations using the Comprehensive Cytogenetic Scoring System (CCSS), the blast count shown as percentage, and the Revised International Prognostic Scoring System (R-IPSS) risk groups (1 – very low).

patient numbers			1	2	3	4	5	6	7	8	9	10	11	12	13	14	15	16	17	18	19	20	21	22	23	24	25	26	27	28
function	gene	(n/%)																												
cohesin	STAG2	0 / 0.0																												
DNA repair	TP53	10 / 35,7			*	*						*	*	*	*							*		*			*			*
chromatin	ASXL1	03.10.2007																*	*	*										
modification	EZH2	02.07.2001													*														*	
DNA	DNMT3A	02.07.2001																				*	*							
methylation	IDH1	01.03.2006							*																					
	IDH2	02.07.2001														*				*										
	TET2	03.10.2007						*									*			*										
RNA splicing	SRSF2	02.07.2001							*									*												
	SF3B1	01.03.2006					*																							
	U2AF1	0 / 0.0																												
signal	ZRSR2	0 / 0.0																												
transduction	BRAF	01.03.2006																									*			
	CALR	0 / 0.0																												
	CBL	02.07.2001																*											*	
	ETKN1	0 / 0.0																												
	CSFR3	0 / 0.0																												
	FLT3	01.03.2006																									*			
	GNAS	0 / 0.0																												
	HRAS	0 / 0.0																												
	JAK2	02.07.2001									*										*									
	KIT	0 / 0.0																												
	KRAS	0 / 0.0																												
	MPL	0 / 0.0																												
	NRAS	0 / 0.0																												
	STAT3	0 / 0.0																												
transcription	CEBPA	01.03.2006		*																										
factors	IKZF1	0 / 0.0																												
	NPM1	01.03.2006		*																										
	SETBP1	03.10.2007													*					*									*	
	RUNX1	01.05.2000																												
total number of mutations/patient			0	2	1	1	1	1	2	0	1	1	1	1	3	1	1	3	1	4	1	2	1	1	0	0	3	0	3	1
CCSS			2	2	5	2	2	3	3	2	2	5	5	5	5	2	3	3	1	3	2	3	3	5	5	3	5	2	3	3
blast count (%)			4	3	7	11	4	7	4	3	3	14	8	3	7	8	9	7	4	4	4	4	9	18	17	8	11	19	14	16
IPSS-R group			2	3	4	2	3	4	4	3	1	5	5	5	5	2	4	4	3	4	3	4	5	5	5	3	5	5	4	5
progress to sAML			no	no	no	no	no	no	no	no	no	no	no	no	no	no	no	no	no	no	no	yes	yes	yes	yes	yes	yes	yes	yes	yes

Preprints (www.preprints.org) | NOT PEER-REVIEWED | Posted: 13 September 2020 doi:10.20944/preprints202009.0280.v1

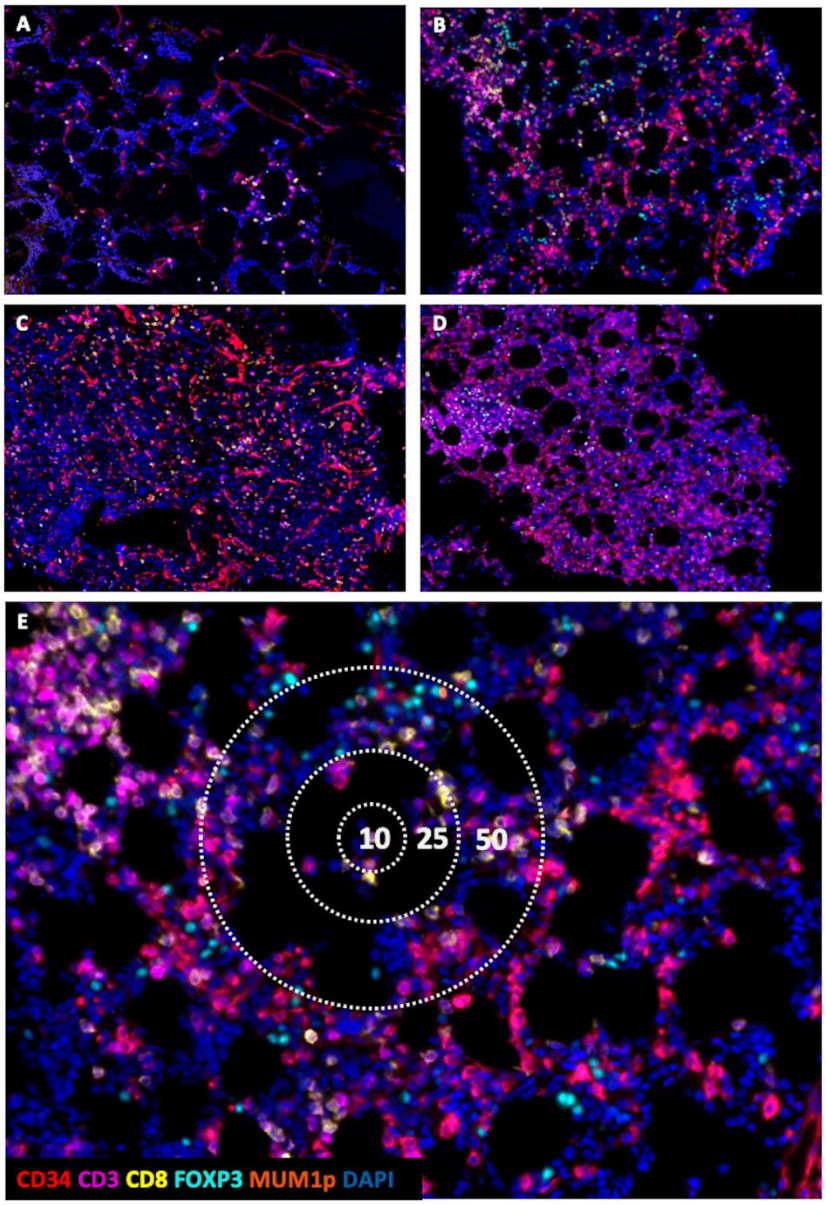

Figure 1: Multicolor analysis of BM biopsies performing MSI

All samples were stained with a six-color panel employing the antibodies CD34 (red), CD3 (pink), CD8 (yellow), FOXP3 (turquoise), MUM1p (orange) and DAPI counterstaining (blue). (A) MDS with multilineage dysplasia without excess of blasts. (B) MDS with excess of blasts 1 (MDS-EB-1). (C) MDS with excess of blasts 2 (MDS-EB-2). (D) Secondary AML with a blast content >30% and myelodysplasia related changes. (E) Intercellular distance algorithm with four applied categories: direct intercellular contact (i), cells within a radius of 10 µm (ii), 25 µm (iii) and 50 µm (iv).

Preprints (www.preprints.org) | NOT PEER-REVIEWED | Posted: 13 September 2020 doi:10.20944/preprints202009.0280.v1

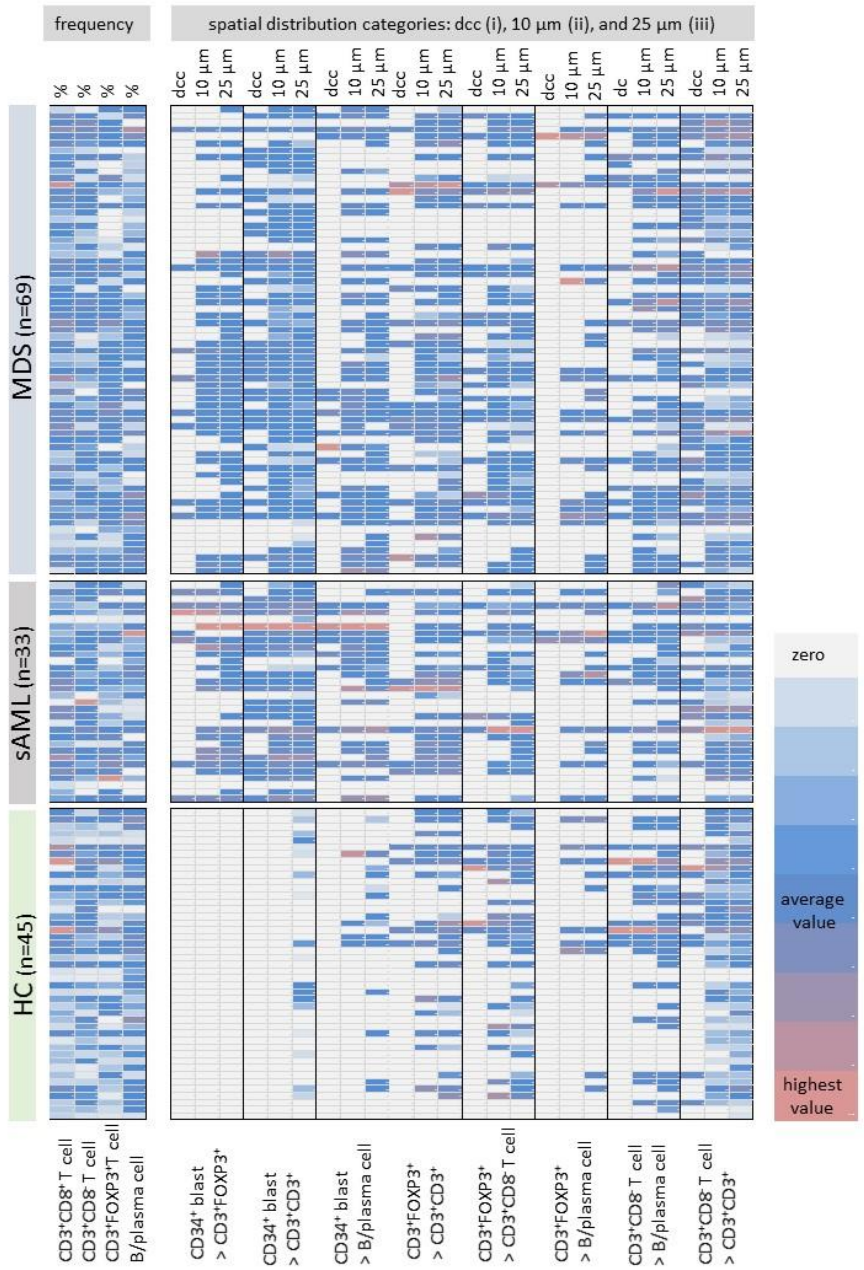

Figure 2: Frequency and the spatial distribution of the respective immune cells analyzed in HC (n=45), MDS (n=69), and sAML (n=33)

The frequencies of $CD3^+CD8^+$ T cells, $CD3^+CD8^-$ T cells, $CD3^+FOXP3^+$ T cells, and $MUM1p^+CD3^-$ B/plasma cells and the spatial distribution of these immune cell subsets to each other and to the $CD34^+$ blasts ($CD34^+$ blasts in relation (>) to $CD3^+FOXP3^+$ T cells, $CD3^+CD8^+$ T cells, $MUM1p^+CD3^-$ B/plasma cells; $CD3^+FOXP3^+$ T cells in relation (>) to $CD3^+CD8^+$ T cells, to $CD3^+CD8^-$ T cells $MUM1p^+CD3^-$ B/plasma cells, and $CD3^+CD8^-$ T cells in relation (>) to $MUM1p^+CD3^-$ B/plasma cells and $CD3^+CD8^-$T cells) are represented in a heat map. All spatial relations are depicted in direct cellular contact (dcc), the 10 µm, and the 25 µm radius. The number of cells in a certain spatial category or the frequency of the immune cells are color-coded, in which white/light grey codes for lowest value, blue codes for average value, and light red codes for highest value of immune cell subsets. Most remarkable is the presence of only

 doi:10.20944/preprints202009.0280.v1

494 few B/plasma cells and no T cell subpopulations in proximity to $CD34^+$ blasts in HC, while the
495 frequency of these immune cell subpopulations is not significantly lower within the bone
496 marrow of MDS compared to sAML samples.

497

Preprints (www.preprints.org) | NOT PEER-REVIEWED | Posted: 13 September 2020 doi:10.20944/preprints202009.0280.v1

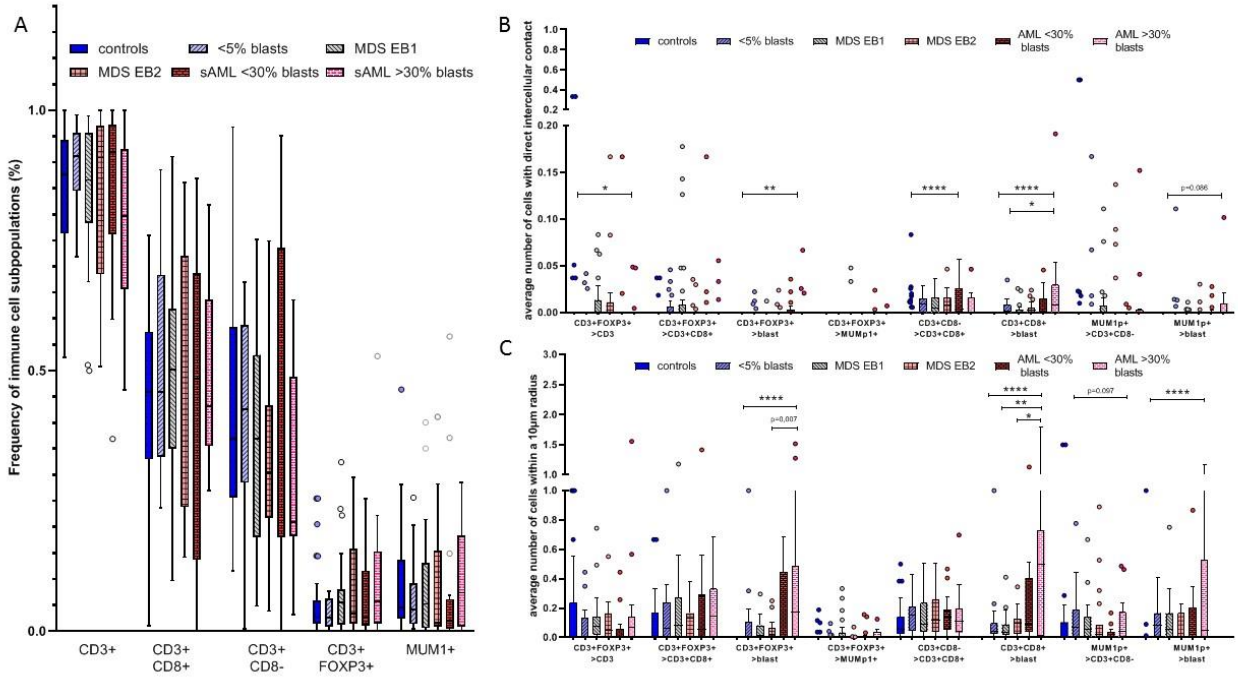

Figure 3: Composition of the immune cell infiltrate with respect to the blast cell count in MDS, and sAML

(A) Evaluation of the frequency of $CD3^+$ T cells, $CD3^+CD8^+$ T-cells, $CD3^+CD8^-$ T cells, $CD3^+FOXP3^+$ T cells, and $MUM1p^+CD3^-$ B/plasma cells as a function of $CD34^+$ blast frequency in BMBs of untreated MDS and sAML patients compared with HCs revealed a significantly elevated frequency of $MUM1p^+CD3^-$ B/plasma cells in AML cases with >30% $CD34^+$ blasts when compared to all other diseased patients. When evaluating the spatial composition by analysis of the different intercellular distances including direct intercellular contact [i], intercellular distance of 10 µm [ii], 25 µm [iii] and 50 µm [iv] the most significant differences were seen considering the distance of 10 µm [ii]. Data are shown for the parameters direct intercellular contact (B) and intercellular distance of 10 µm (C). Both, $CD3^+FOXP3^+$ and $CD3^+CD8^-$ T cells were significantly more frequent in the AML cases with >30% blasts compared to all other groups. In addition, the frequency of these cells in neighborhood of $CD34^+$ cells was significantly higher when compared to healthy controls and stable within the MDS subgroups and the AML cases with <30% blasts. Also, a significant higher frequency of $MUM1p^+CD3^-$ B/plasma cells was seen in the group of AML cases >30% and also in the AML 20-30% blast group.

Preprints (www.preprints.org) | NOT PEER-REVIEWED | Posted: 13 September 2020 doi:10.20944/preprints202009.0280.v1

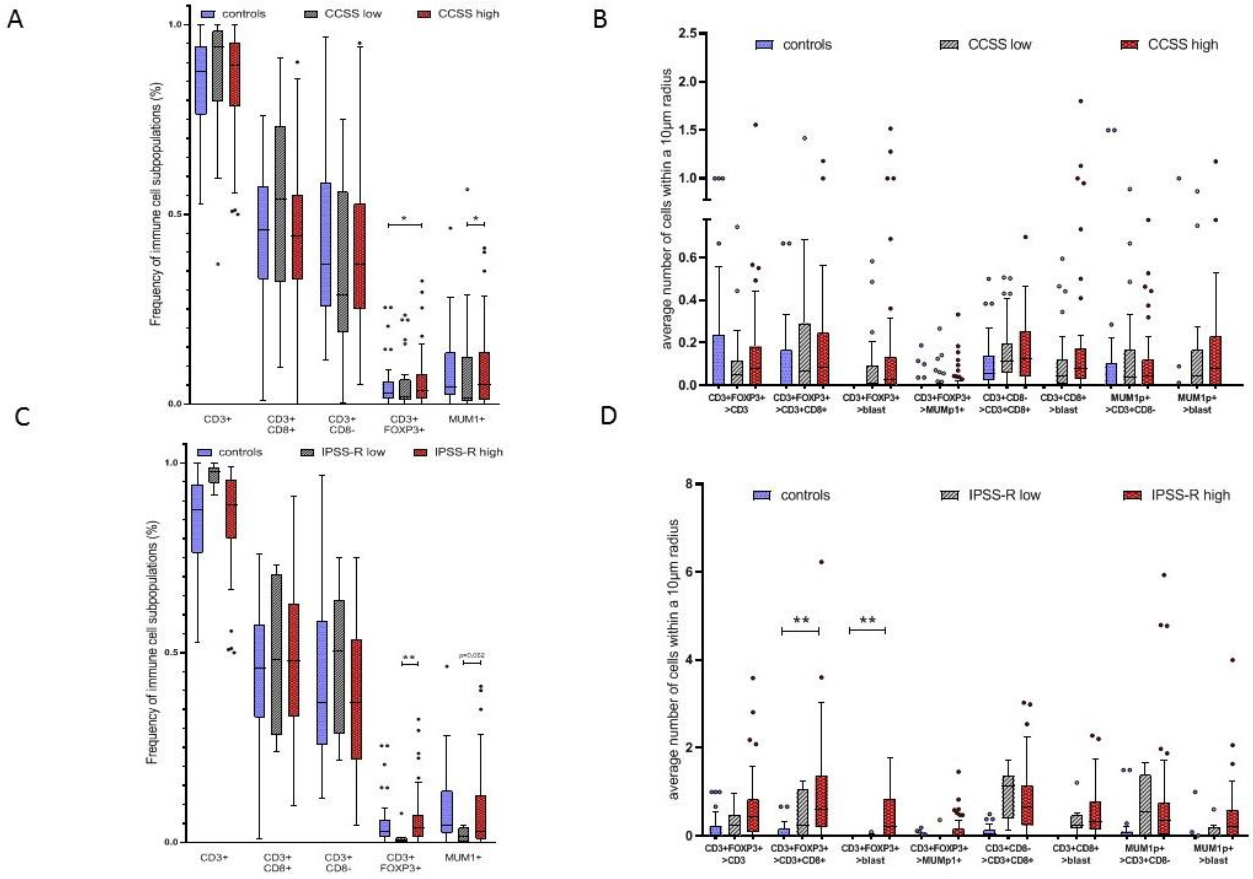

Figure 4: Altered composition of the immune cell infiltrate and bone marrow blasts in MDS/sAML depending on the karyotype and the IPSS-R due to immune cell subset frequencies, and spatial distribution

(A) Higher risk cytogenetic aberrations were connected to significantly increased levels of MUM1p$^+$CD3$^-$ post–germinal center B cells / plasma cells and CD3$^+$FOXP3$^+$ T cells. Spatial analysis data for CCSS high versus CCSS low untreated MDS specimen regarding (B) cells within a radius of 10 µm [ii] revealed no significant differences concerning the CCSS high versus CCSS low prognostic group. (C) Higher IPSS-R risk group (intermediate, high, and very high risk) showed significantly increased levels of CD3$^+$FOXP3$^+$ T cells and slightly increased numbers of MUM1p$^+$CD3$^-$ B/plasma cells. (D) Spatial analysis data for IPSS-R high versus IPSS-R low untreated MDS specimen regarding cells within a radius of 10 µm revealed no significant differences.

Preprints (www.preprints.org) | NOT PEER-REVIEWED | Posted: 13 September 2020 doi:10.20944/preprints202009.0280.v1

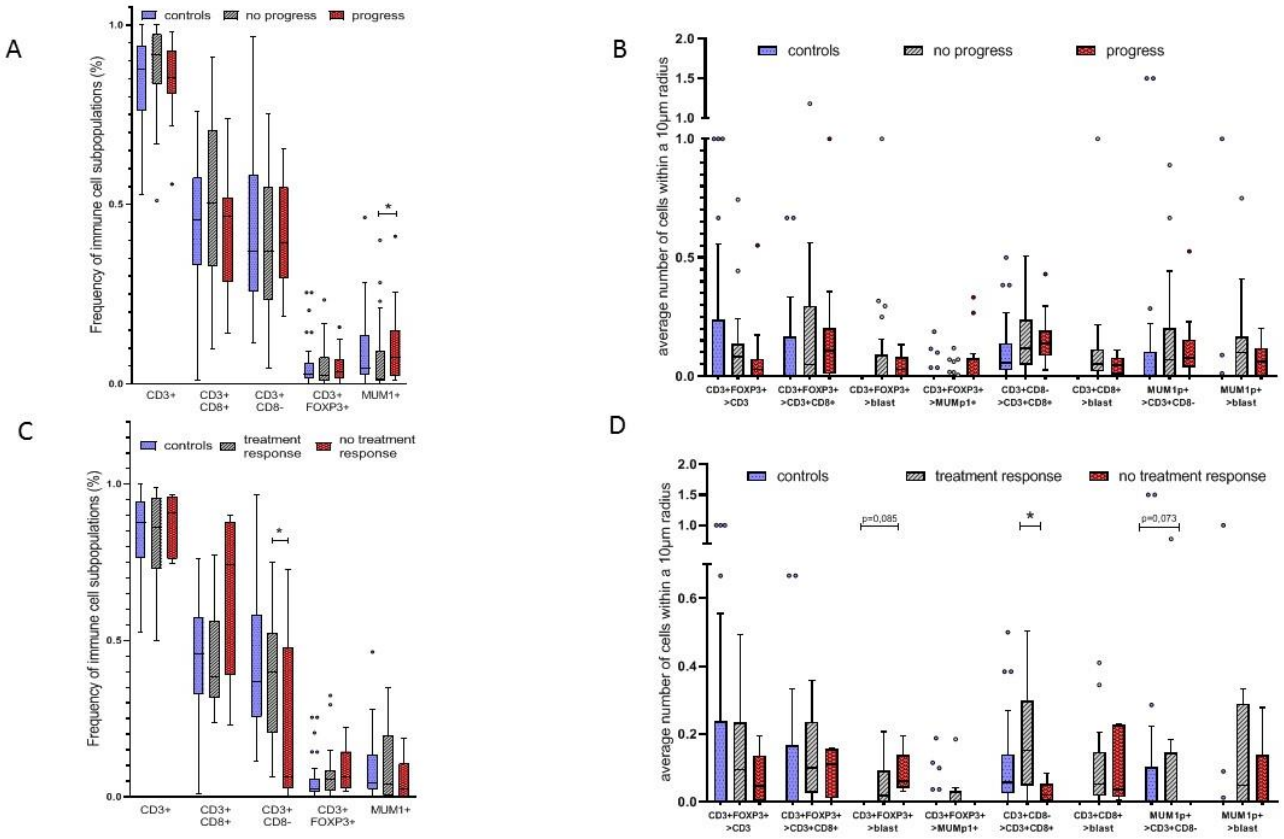

Figure 5: Altered composition of the immune cell infiltrate with the clinical course of MDS in untreated patients and patients that received HMA treatment

Tukey plots of (A) subpopulation frequencies in untreated patients as well as their spatial distribution regarding (B) the 10 µm radius [ii] are shown and revealed no significant differences. (C) In MDS samples of patients that received prior HMA treatment, patients with treatment response showed significantly increased numbers of $CD3^+CD8^+$ T cells in the BM. (D) In this patient subgroup significantly more T cell subsets and $MUM1p^+CD3^-$ B/plasma cells are located in close proximity within the 10 µm radius compared to patients in whom HMA treatment failed.

References

1. Corey SJ, Minden MD, Barber DL, Kantarjian H, Wang JCY, Schimmer AD. Myelodysplastic syndromes: the complexity of stem-cell diseases. Nat Rev Cancer. 2007 Feb;7(2):118–29.

2. Steensma DP, Bejar R, Jaiswal S, Lindsley RC, Sekeres MA, Hasserjian RP, et al. Clonal hematopoiesis of indeterminate potential and its distinction from myelodysplastic syndromes. Blood. 2015 Jul 2;126(1):9–16.

3. Ghobrial IM, Detappe A, Anderson KC, Steensma DP. The bone-marrow niche in MDS and MGUS: implications for AML and MM. Nat Rev Clin Oncol. 2018 Jan 9;15(4):219–33.

4. Greenberg PL. Molecular and genetic features of myelodysplastic syndromes. Int J Lab Hematol. 2012 Jun;34(3):215–22.

5. Greenberg PL, Tuechler H, Schanz J, Sanz G, Garcia-Manero G, Sole F, et al. Revised International Prognostic Scoring System for Myelodysplastic Syndromes. Blood. 2012 Sep 20;120(12):2454–65.

6. Esplin BL, Shimazu T, Welner RS, Garrett KP, Nie L, Zhang Q, et al. Chronic Exposure to a TLR Ligand Injures Hematopoietic Stem Cells. J Immunol. 2011 May 1;186(9):5367–75.

7. Komrokji RS, Kulasekararaj A, Al Ali NH, Kordasti S, Bart-Smith E, Craig BM, et al. Autoimmune diseases and myelodysplastic syndromes. Am J Hematol. 2016 May;91(5):E280-283.

8. Glenthøj A, Ørskov AD, Hansen JW, Hadrup SR, O'Connell C, Grønbæk K. Immune Mechanisms in Myelodysplastic Syndrome. Int J Mol Sci. 2016 Jun 15;17(6).

9. Hofmann W-K. Characterization of gene expression of CD34+ cells from normal and myelodysplastic bone marrow. Blood. 2002 Nov 15;100(10):3553–60.

10. Pellagatti A, Cazzola M, Giagounidis A, Perry J, Malcovati L, Della Porta MG, et al. Deregulated gene expression pathways in myelodysplastic syndrome hematopoietic stem cells. Leukemia. 2010 Apr;24(4):756–64.

11. Anderson LA, Pfeiffer RM, Landgren O, Gadalla S, Berndt SI, Engels EA. Risks of myeloid malignancies in patients with autoimmune conditions. Br J Cancer. 2009 Mar;100(5):822–8.

12. Fozza C. The burden of autoimmunity in myelodysplastic syndromes. Hematol Oncol. 2018 Feb;36(1):15–23.

13. Kristinsson SY, Björkholm M, Hultcrantz M, Derolf ÅR, Landgren O, Goldin LR. Chronic Immune Stimulation Might Act As a Trigger for the Development of Acute Myeloid Leukemia or Myelodysplastic Syndromes. J Clin Oncol. 2011 Jul 20;29(21):2897–903.

14. Schanz J, Tüchler H, Solé F, Mallo M, Luño E, Cervera J, et al. New Comprehensive Cytogenetic Scoring System for Primary Myelodysplastic Syndromes (MDS) and Oligoblastic Acute Myeloid Leukemia After MDS Derived From an International Database Merge. J Clin Oncol. 2012 Mar 10;30(8):820–9.

15. Wang C, Yang Y, Gao S, Chen J, Yu J, Zhang H, et al. Immune dysregulation in myelodysplastic syndrome: Clinical features, pathogenesis and therapeutic strategies. Crit

584 Rev Oncol Hematol. 2018 Feb;122:123–32.

585 16. Kotsianidis I, Bouchliou I, Nakou E, Spanoudakis E, Margaritis D, Christophoridou
586 AV, et al. Kinetics, function and bone marrow trafficking of CD4+CD25+FOXP3+ regulatory T
587 cells in myelodysplastic syndromes (MDS). Leukemia. 2009 Mar;23(3):510–8.

588 17. Kordasti SY, Afzali B, Lim Z, Ingram W, Hayden J, Barber L, et al. IL-17-producing
589 CD4(+) T cells, pro-inflammatory cytokines and apoptosis are increased in low risk
590 myelodysplastic syndrome. Br J Haematol. 2009 Apr;145(1):64–72.

591 18. Mailloux AW, Sugimori C, Komrokji RS, Yang L, Maciejewski JP, Sekeres MA, et al.
592 Expansion of Effector Memory Regulatory T Cells Represents a Novel Prognostic Factor in
593 Lower Risk Myelodysplastic Syndrome. J Immunol. 2012 Sep 15;189(6):3198–208.

594 19. Lopes MR, Traina F, Campos P de M, Pereira JKN, Machado-Neto JA, Machado H
595 da C, et al. IL10 inversely correlates with the percentage of CD8+ cells in MDS patients.
596 Leuk Res. 2013 May;37(5):541–6.

597 20. Maratheftis CI, Andreakos E, Moutsopoulos HM, Voulgarelis M. Toll-like Receptor-4 Is
598 Up-Regulated in Hematopoietic Progenitor Cells and Contributes to Increased Apoptosis in
599 Myelodysplastic Syndromes. Clin Cancer Res. 2007 Feb 15;13(4):1154–60.

600 21. Kuninaka N, Kurata M, Yamamoto K, Suzuki S, Umeda S, Kirimura S, et al.
601 Expression of Toll-like receptor 9 in bone marrow cells of myelodysplastic syndromes is
602 down-regulated during transformation to overt leukemia. Exp Mol Pathol. 2010
603 Apr;88(2):293–8.

604 22. Wei Y, Dimicoli S, Bueso-Ramos C, Chen R, Yang H, Neuberg D, et al. Toll-like
605 receptor alterations in myelodysplastic syndrome. Leukemia. 2013 Sep;27(9):1832–40.

606 23. Mährle T, Akyüz N, Fuchs P, Bonzanni N, Simnica D, Germing U, et al. Deep
607 sequencing of bone marrow microenvironments of patients with del(5q) myelodysplastic
608 syndrome reveals imprints of antigenic selection as well as generation of novel T-cell clusters
609 as a response pattern to lenalidomide. Haematologica. 2019 Jul;104(7):1355–64.

610 24. Weltgesundheitsorganisation. WHO classification of tumours of haematopoietic and
611 lymphoid tissues. Revised 4th edition. Swerdlow SH, Campo E, Harris NL, Jaffe ES, Pileri
612 SA, Stein H, et al., editors. Lyon: International Agency for Research on Cancer; 2017. 585 p.
613 (World Health Organization classification of tumours).

614 25. Wickenhauser C, Bethmann D, Feng Z, Jensen SM, Ballesteros-Merino C, Massa C,
615 et al. Multispectral Fluorescence Imaging Allows for Distinctive Topographic Assessment and
616 Subclassification of Tumor-Infiltrating and Surrounding Immune Cells. Methods Mol Biol
617 Clifton NJ. 2019;1913:13–31.

618 26. Bauer M, Vaxevanis C, Bethmann D, Massa C, Pazaitis N, Wickenhauser C, et al.
619 Multiplex immunohistochemistry as a novel tool for the topographic assessment of the bone
620 marrow stem cell niche. Methods Enzymol. 2020;635:67–79.

621 27. Ivy KS, Brent Ferrell P. Disordered Immune Regulation and its Therapeutic Targeting
622 in Myelodysplastic Syndromes. Curr Hematol Malig Rep. 2018;13(4):244–55.

623 28. Takeuchi O, Akira S. Pattern Recognition Receptors and Inflammation. Cell. 2010
624 Mar;140(6):805–20.

625 29. Ma S, Wan X, Deng Z, Shi L, Hao C, Zhou Z, et al. Epigenetic regulator CXXC5
626 recruits DNA demethylase Tet2 to regulate TLR7/9-elicited IFN response in pDCs. J Exp

627 Med. 2017 01;214(5):1471–91.

628 30. Feng Z, Bethmann D, Kappler M, Ballesteros-Merino C, Eckert A, Bell RB, et al.
629 Multiparametric immune profiling in HPV- oral squamous cell cancer. JCI Insight. 2017 Jul
630 20;2(14).

631 31. Barua S, Fang P, Sharma A, Fujimoto J, Wistuba I, Rao AUK, et al. Spatial interaction
632 of tumor cells and regulatory T cells correlates with survival in non-small cell lung cancer.
633 Lung Cancer Amst Neth. 2018;117:73–9.

634 32. Ema H, Suda T. Two anatomically distinct niches regulate stem cell activity. Blood.
635 2012 Sep 13;120(11):2174–81.

636 33. Ding L, Saunders TL, Enikolopov G, Morrison SJ. Endothelial and perivascular cells
637 maintain haematopoietic stem cells. Nature. 2012 Jan 25;481(7382):457–62.

638 34. Zhang Q, Zhao K, Shen Q, Han Y, Gu Y, Li X, et al. Tet2 is required to resolve
639 inflammation by recruiting Hdac2 to specifically repress IL-6. Nature. 2015 Sep
640 17;525(7569):389–93.

641 35. Medyouf H, Mossner M, Jann J-C, Nolte F, Raffel S, Herrmann C, et al.
642 Myelodysplastic Cells in Patients Reprogram Mesenchymal Stromal Cells to Establish a
643 Transplantable Stem Cell Niche Disease Unit. Cell Stem Cell. 2014 Jun;14(6):824–37.

644 36. Moore KA, Lemischka IR. "Tie-ing" down the Hematopoietic Niche. Cell. 2004
645 Jul;118(2):139–40.

646 37. Chen S, Zambetti NA, Bindels EMJ, Kenswill K, Mylona AM, Adisty NM, et al.
647 Massive parallel RNA sequencing of highly purified mesenchymal elements in low-risk MDS
648 reveals tissue-context-dependent activation of inflammatory programs. Leukemia. 2016
649 Sep;30(9):1938–42.

650 38. Zhang J, Niu C, Ye L, Huang H, He X, Tong W-G, et al. Identification of the
651 haematopoietic stem cell niche and control of the niche size. Nature. 2003 Oct
652 23;425(6960):836–41.

653 39. Raaijmakers MHGP, Mukherjee S, Guo S, Zhang S, Kobayashi T, Schoonmaker JA,
654 et al. Bone progenitor dysfunction induces myelodysplasia and secondary leukaemia.
655 Nature. 2010 Apr;464(7290):852–7.

656 40. Zhou X, Liao W-J, Liao J-M, Liao P, Lu H. Ribosomal proteins: functions beyond the
657 ribosome. J Mol Cell Biol. 2015 Apr;7(2):92–104.

658 41. Mekinian A, Braun T, Decaux O, Falgarone G, Toussirot E, Raffray L, et al.
659 Inflammatory Arthritis in Patients With Myelodysplastic Syndromes: A Multicenter
660 Retrospective Study and Literature Review of 68 Cases. Medicine (Baltimore). 2014
661 Jan;93(1):1–10.

662 42. de Hollanda A, Beucher A, Henrion D, Ghali A, Lavigne C, Lévesque H, et al.
663 Systemic and immune manifestations in myelodysplasia: A multicenter retrospective study.
664 Arthritis Care Res. 2011 Aug;63(8):1188–94.

665 43. DiNardo CD, Garcia-Manero G, Pierce S, Nazha A, Bueso-Ramos C, Jabbour E, et
666 al. Interactions and relevance of blast percentage and treatment strategy among younger
667 and older patients with acute myeloid leukemia (AML) and myelodysplastic syndrome (MDS):
668 The Relevance of Blast% in MDS and AML. Am J Hematol. 2016 Feb;91(2):227–32.

669 44. Kittang AO, Kordasti S, Sand KE, Costantini B, Kramer AM, Perezabellan P, et al.

670 Expansion of myeloid derived suppressor cells correlates with number of T regulatory cells
671 and disease progression in myelodysplastic syndrome. Oncoimmunology. 2016
672 Feb;5(2):e1062208.

673 45. Barreyro L, Chlon TM, Starczynowski DT. Chronic immune response dysregulation in
674 MDS pathogenesis. Blood. 2018 Oct 11;132(15):1553–60.

675 46. Uy GL, Duncavage EJ, Chang GS, Jacoby MA, Miller CA, Shao J, et al. Dynamic
676 changes in the clonal structure of MDS and AML in response to epigenetic therapy.
677 Leukemia. 2017 Apr;31(4):872–81.

678 47. Lindblad KE, Goswami M, Hourigan CS, Oetjen KA. Immunological effects of
679 hypomethylating agents. Expert Rev Hematol. 2017 Aug 3;10(8):745–52.

680 48. Costantini B, Kordasti SY, Kulasekararaj AG, Jiang J, Seidl T, Abellan PP, et al. The
681 effects of 5-azacytidine on the function and number of regulatory T cells and T-effectors in
682 myelodysplastic syndrome. Haematologica. 2013 Aug 1;98(8):1196–205.

683